A HIGH PERFORMANCE OA-TOF MASS SPECTROMETER FOR ACCURATE MASS MEASUREMENT OF MOBILITY SEPARATED IONS

Jakub Ujma, Jason Wildgoose, Martin R. Green, Kevin Giles, Nick Tomczyk
Waters Corporation, Stamford Avenue, Altrincham Road, Wilmslow, UK

OVERVIEW

- **A new Q-Cyclic IM-ToF research platform**
- **A novel "offset W mode" ToF geometry**
- **ToF resolution ~120,000 (W) and ~65,000 (V)**
- **IM-ToF transfer optics capable of maintaining the temporal fidelity of IM peaks with widths <200 µs**
- **High resolution Q-IM-CID-ToF data show minimal IM peak distortion during activation**

INTRODUCTION

The benefits of coupling Ion Mobility (IM) separation devices to ToF-MS are well established with instruments utilising these technologies now commercially available. The strength of ToF mass analysers in these geometries is their inherent speed, allowing multiple complete mass spectra to be acquired across ion mobility peaks. Whilst the separation timescales of ToF-MS are well suited to IMS, significant challenges exist in conditioning the ion beam for optimum ToF performance whilst maintaining the fidelity of the IM separation. In addition the temporal concentrating effects of IM raise significant challenges for the acquisition system. Here, we present a novel combination of beam conditioning ion optics, ToF geometry and acquisition system that alleviates these issues.

INSTRUMENT DESIGN

The instrument outline is presented in Figure 1. Ions are generated in an electrospray ionisation source and transferred through the first vacuum stages of the spectrometer using two travelling wave (T-wave) RF confining ion guides (StepWave, **a**, **b**), which propel ions towards the quadrupole mass filter (**c**). The subsequent RF confining gas cell (**d**, Argon, 3e-2 mBar) allows trapping and activation of mass selected ions. The resulting ion packets are then transported through a low pressure guide (**e,** 5e-3 mBar) and into a RF confining cell filled with Helium (**f**, 2 mBar) and subsequent RF/DC ion guide (**g**) operating in Nitrogen at a similar pressure. Following this, there is an RF confining, planar array of electrodes (**h**) forming part of an orthogonal closed loop the cyclic T-wave IM device (**i**, 1.8 mBar Nitrogen, 1 m). The T-wave direction in the array can be altered to either match those in the orthogonal IM device or to inject/eject ions from it (see poster 37 for details). Post IM device, ions are transported through a RF/DC ion guide (**j**, IM pressure), through a low pressure RF/DC guide (**k,** 5e-3 mBar) into an 'RF only' segmented quadrupole gas cell (**l**, Argon, 2e-2 mBar) with a superimposed DC field. The quadrupolar field reduces the initial 'phase space' of the ion beam while the DC field acts to maintain mobility separation. Both field components help to improve the relationship between ToF resolution and sensitivity. The orthogonal acceleration ToF (**m**-**r**) includes an extension (**s**) to the standard oa-ToF of the Synapt instrument. The resulting offset V/W geometry provides 40/120 cm longer flight path respectively. The increased physical separation of the pusher optics (**n**) and detector (**r**) effectively improves the stability of the high voltages simplifying the relationship between time of flight and m/z. Overall, the system enables m/z measurements at resolutions greater than 100,000 FWHM (Figure 2A) at better than 95% transmission through the transfer optics. When combined with the extended flight times and the wide dynamic range ADC acquisition electronics [2] the system can provide sub ppm accurate m/z measurements for fast chromatographic separations as shown in figure 2B.

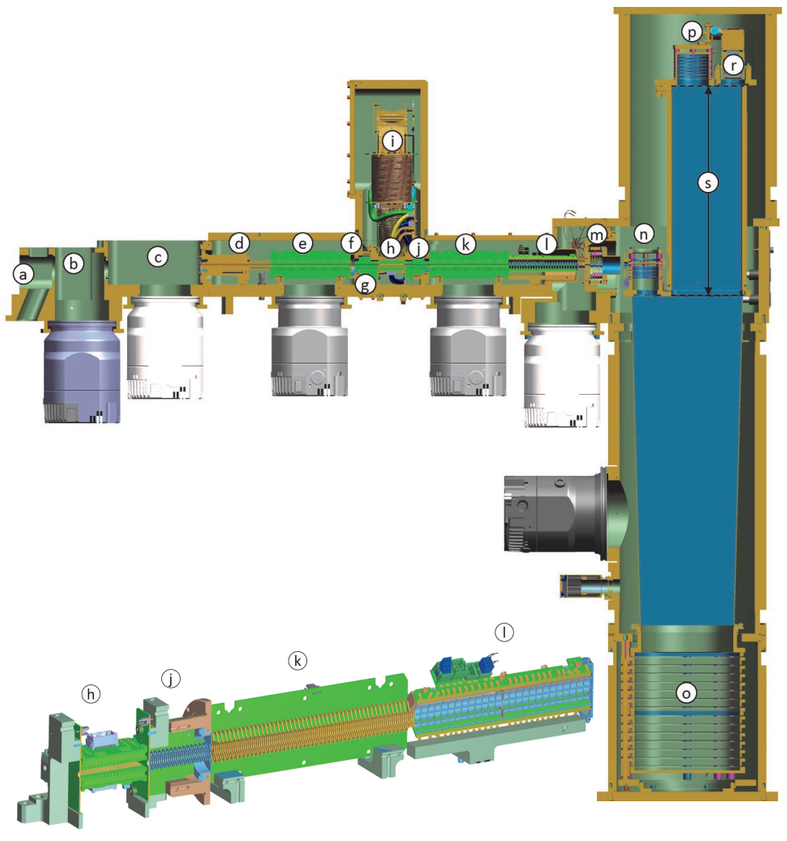

*Figure 1. Instrument schematic. **a**: ESI / Stepwave source, **b**: 2nd StepWave guide, **c**: quadrupole, **d**: trap collision cell, **e**: low pressure ion guide, **f**: helium cell, **g**: pre array guide, **h**: electrode array, **i**: cyclic IMS, **j**: post array guide, **k**: low pressure guide, **l**: segmented quadrupole collision cell, **m**: ToF transfer optics, **n**: pusher, **o**: reflectron, **p**: W mode reflectron, **r**: detector, **s**: ToF extension.*

TOF RESOLUTION AND MASS ACCURACY

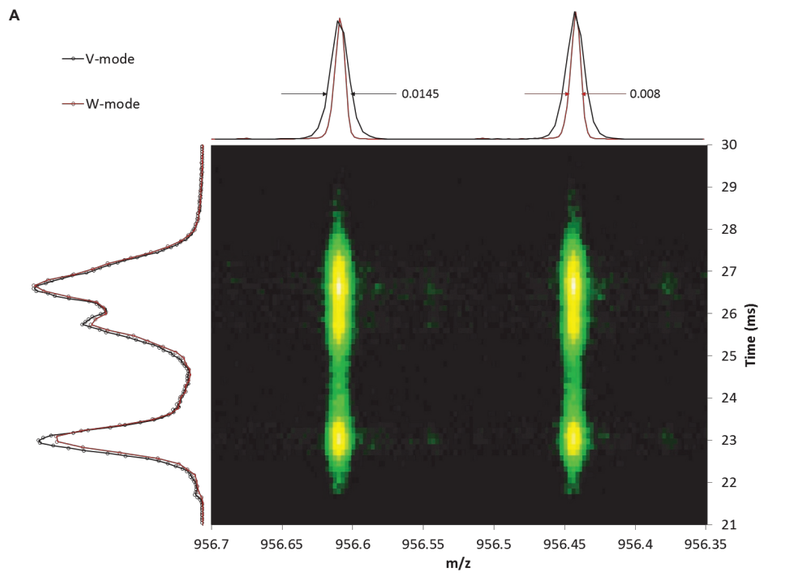

*Figure 2. ToF resolution and mass accuracy. (**A**) 2D IM-ToF spectrum of Bovine Insulin (6+) at 1 pass around the cyclic IMS measured in V-mode (black traces, R ~65,000) and W-mode (red traces, R~ 120,000). IM resolution of ~70 Ω/ΔΩ was measured using singly charged GRGDS/SDGRG peptides at similar instrument parameters. (**B**) Summary of 5 replicate injections for identification of Reserpine. 10min generic LC-HDMSE method with 1 pass around cyclic IMS. Data were externally calibrated with Sodium Formate and LockMass correction applied during processing in UNIFI 1.8.1. Data shows an RMS error of 0.93 ppm for the Reserpine precursor.*

IM-TOF TRANSFER OPTICS PERFORMANCE

The desired characteristics of the ion optics between the IM and ToF analysers is the ability to maintain the temporal fidelity of IM separated peaks during transfer through gas cell, activation and beam conditioning. Here, we assess the above by utilising custom programmable functions of the electrode array (Figure 1**h**, Poster 37, and [1]) to eject ions into the ToF analyser. After 1 pass around the cyclic IM, a section of the arrival time distribution (ATD) is ejected (Figure 3A-C, red traces).

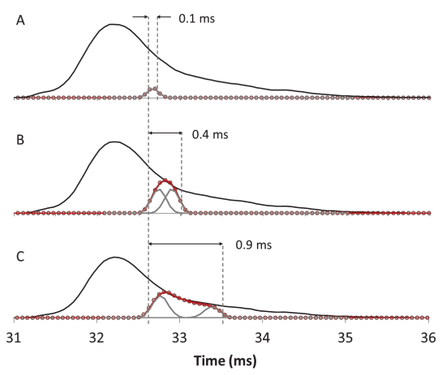

For the shortest ejection time setting (Figure 3A), the arriving peaks can be approximated with a Gaussian distribution. The measured FWHM is comparable to the ejection time setting. For the longer ejection times, the measured ATDs are no longer symmetric and begin to resemble shape of the "parent" ATD convoluted with Gaussian-like rising and falling edges (Figure 3B and C, grey traces).

*Figure 3. ATDs of Bovine Insulin (6+) after 1 pass around the cyclic IMS. A segment of ions is ejected from the gate array for 0.1 ms (**A**), 0.4 ms (**B**) and 0.9 ms (**C**). Black traces represent unmodified "parent" ATDs. Red traces represent ejected section. Grey traces indicate Gaussian peaks fitted to rising and falling edges of ejected sections. Dashed lines represent ejection width aligned with ATDs.*

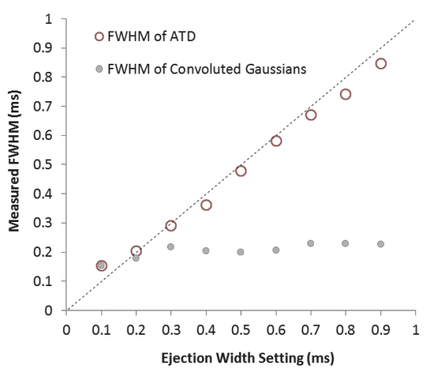

The FWHM of the convoluted Gaussians appear constant (~0.2 ms) across the ejection width setting range (Figure 4, grey dots). FWHMs of the measured ATDs (red circles) are comparable with the ejection width setting, indicating no significant distortions. The minimum measureable peak width (limited by post IM broadening) is around 0.1-0.2 ms.

Figure 4. FWHM of arrival time distributions and convoluted Gaussians vs ejection width setting. Measured FWHM of the ATD corresponds to FWHM of convoluted Gaussians + difference of their means.

CID OF MOBILITY SEPARATED IONS

Post IM activation can have a deleterious effect on the temporal fidelity of recorded ATDs and can introduce shifts in the recorded times. Here, we investigate both effects using isobaric species (reverse peptides SDGRG, GRGDS, 1+) with very similar collision cross sections (205.3 Å^2 and 208.5 Å^2). The most abundant fragments of earlier and later arriving isobaric precursor ions are observed at m/z 404 and m/z 289 respectively (Figure 5). We compare ATDs of those "diagnostic" fragment peaks to ATD of parent ions to assess the extent of possible broadening and time shift upon activation.

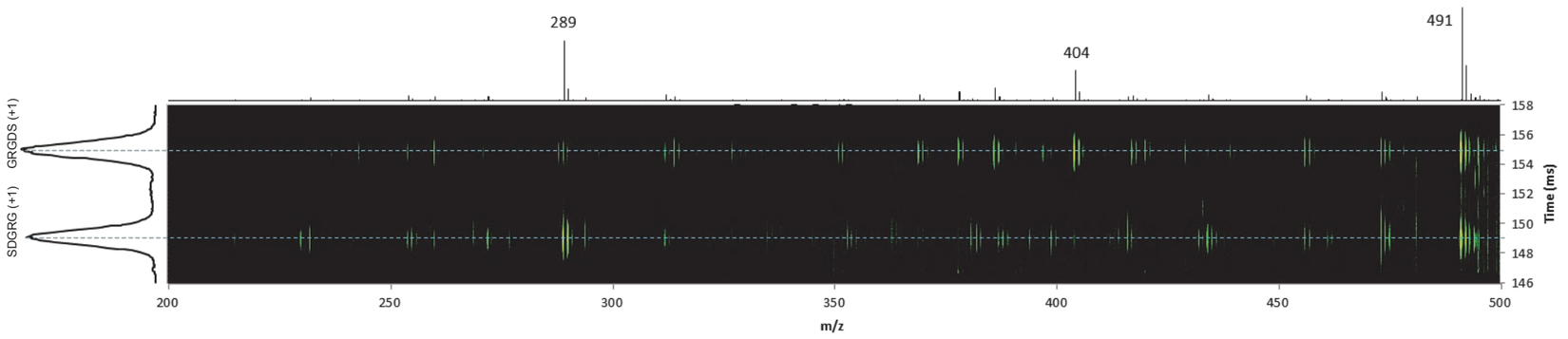

Figure 5 (above). 2D IM-CID-ToF spectrum of peptide mixture (SDGRG, GRGDS, 1+). The m/z of interest is selected using the quadrupole mass filter, subject to IM separation (15 passes, ~300 Ω/ΔΩ), activated with 18eV of post IMS collision energy and measured in ToF V mode, (R~60,000).

Figure 6 (left) illustrates the magnitude of the ATD shift and width distortion due to post IMS activation for ions subject to 1 and 3 passes around cyclic IM. We note that FWHM measured for fragments appear marginally narrower compared to FWHM of parent ions. The magnitude of the ATD shift is ~30 µs for parent ions and ~50 µs for fragments (for other collision energies refer to Figure 7). We attribute that difference to the difference in mobility (and m/z) of parents and fragments. Expectedly, the ATD shift is constant across data acquired for different number of passes around the cyclic IMS. As a consequence the % error in time measurement due to activation decrease with number of passes (~0.2% for 1 pass, ~0.1% for 3 passes and ~0.03% for 15 passes).

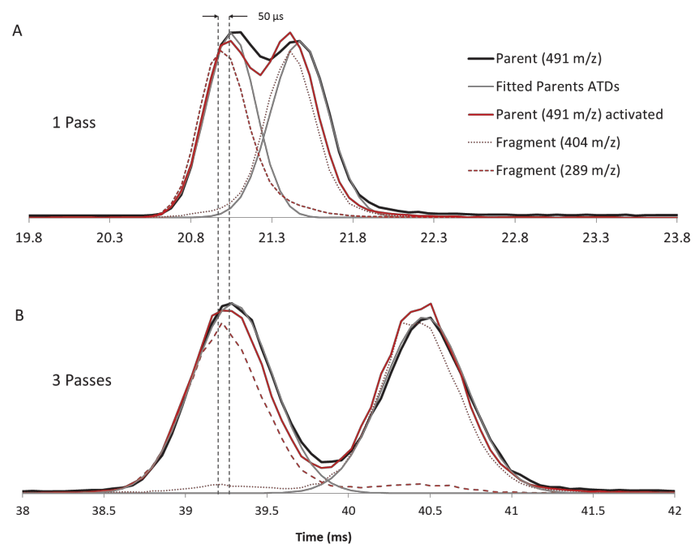

*Figure 6. ATDs peptide mixture (SDGRG, GRGDS 1+) subject to IM separation: (**A**) 1 pass, (**B**) 3 passes; and activated with 18eV of collision energy.*

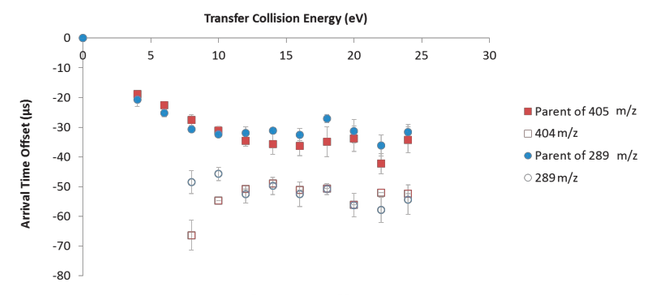

Figure 7. Magnitude of ATD offsets due to activation in collision cell vs activation energy.

CONCLUSION

- **We present high resolution ToF data (V mode ~65,000, W mode ~120,000) obtained for ions separated at high IM resolution (70-300 Ω/ΔΩ) with sub ppm m/z accuracy.**
- **We discuss the instrument performance in terms of maintaining high fidelity IM separations during transmission of packets from the IM into the ToF analyser and IM-CID-ToF experiments.**
- **We focus on IM separations at low number of passes (narrow ATDs) in order to exaggerate potential effects of ATD broadening/distortion. Already minor in the above data, both deleterious effects diminish further at high number of IM passes.**

Special thanks to entire project team at Waters Wilmslow:

Bharat Chande, Praveen Harapanahalli, James Harrison, Darren Hewitt, John Iveson, David Langridge, John Lewis, Witold Niklewski, Mark Pickering, Keith Richardson, Sandra Richardson, Graham Scambler, Chris Wheeldon.

References

1. Giles et al, Characterising a T-Wave Enabled Multi-pass Cyclic Ion Mobility Separator, ASMS 2015 Proceedings, St Louis
2. Green et al, A Novel Wide Dynamic Range oa-ToF Detection System Based on Dual 10-bit ADCs and FPGA Processing, ASMS 2016 Proceedings, San Antonio

TO DOWNLOAD A COPY OF THIS POSTER, VISIT WWW.WATERS.COM/POSTERS